

Was the flare on 5 July 1989 a white light flare?

K.J. Li^{1,2} and S.H. Zhong²

¹ CCAST (World Laboratory), P.O. Box 8730, Beijing 100080, China

² Yunnan Observatory, Chinese Academy of Sciences, Yunnan 650011, China

Received 18 July 1994 / Accepted 27 October 1996

Abstract. The continuous emission spectra of $H\alpha$, $H\beta$, and $H\gamma$ wave bands of the solar flare of 5 July 1989 have been analysed. We demonstrate that the flare not only emits at the line centres and wings of $H\alpha$, $H\beta$, and $H\gamma$, but also in the continuum near these lines. The positions, durations, and configurations of the four flare kernels are respectively similar to those of a white light flare (WLF). Therefore we conclude that this flare was very likely a WLF. The magnetic field of the active region has also been analysed. Most of the flare is located in the vicinity of the neutral line of the magnetic field. Three of the four flare kernels that have continuous emissions lie in the penumbrae of the preceding sunspot and the following sunspot, and near the neutral line, where the magnetic field shears, twists, and shows evidences of having been squeezed or compressed. The fourth kernel of the flare is located in the photospheric region near a small sunspot (about $4''$ in size). The flare kernel with the brightest continuous emission is located at a point where the gradient of the longitudinal magnetic field has maximum value (0.52 Gs/Km). Thus the magnetic field at the flare kernels is of two kinds: one showing twist, shear, and possible compression, the other in the photospheric region near a sunspot group or a sunspot. The total energy of the flare is estimated to be about 3.8×10^{30} erg.

Key words: Sun: activity – Sun: flare – Sun: magnetic fields

1. Introduction

White light flares are defined as those flares which produce significant enhancement of emission in the visible light continuum and can be seen in white light under the quite bright background of the solar surface (Wang et al. 1986; Xuan et al. 1992). WLFs are extremely rare and violent solar activities. WLFs occur at a rate ≈ 15 per year near the solar maximum (Neidig & Cliver 1983). Earlier studies showed that only 61 WLFs had been observed since 1 Sep. 1959, as determined from white light, broad-band photographic or spectrographic observations. The most recent statistical data show that the number has risen to 86 (Neidig & Wiborg 1993), still far less than the theoretically

estimated number, so it is necessary to search for WLFs in the obtained flare data.

Among the known WLF events, there are only a few spectral data from which one can obtain important parameters. These data show that: (i) WLFs and common optical flares have: (a) identical characteristics for line-centre emissions of $H\alpha$, $H\beta$, $H\gamma$, etc. and (b) different characteristics on line-wing emissions of these lines. Continuum emissions of WLFs are very broad ($\geq 20 \text{ \AA}$), but continuum emissions of common optical flares are generally very narrow; (ii) the maximum emission power of WLFs can reach 10^{28} J s^{-1} , 2 or 3 orders of magnitude higher than that of $H\alpha$ flares (Slonim & Korobova 1975; Neidig & Wiborg 1993); (iii) WLFs produce the extreme density conditions attained in solar optical flares, similar in many respects to stellar flares (Worden 1983; Xuan et al. 1992). Therefore the spectral data of WLFs are very important. More observations are necessary.

WLFs are of great importance in flare research and present a great challenge to solar atmospheric models and energy transport mechanisms (Lites & Cook 1979; Machado et al. 1980; Bumba & Gesztelyi 1988; Neidig 1989). Morphologies of WLFs are far from being understood. Some important parameters in the kernels with strong emissions remain unknown. One cannot explain the observations of WLFs by using the present theoretical models of flares. Therefore, WLFs have attracted increasing attention from solar physicists.

On 5 July 1989, a flare ($N22^0, E37^0$) occurred in NOAA AR5575. Photographic data of two-dimensional multi-band spectra and synchronous $H\alpha$ filtergrams were obtained of this flare. Data of the sunspot group in AR5575 and the magnetic field of the active region on that day were obtained as well. In this paper, the flare is identified to be a WLF, and the magnetic field of the active region which enclosed the flare is analysed.

2. Observations

On 5 July 1989, an $H\alpha$ flare ($N22^0E37^0$) in the active region NOAA/USAF 5575 occurred from 0753UT to 0829UT (CSGD 1989; NOAA 1990). From 0758UT to 0807UT, we observed it and obtained its two-dimensional spectral data of the $H\alpha$, $H\beta$, $H\gamma$ bands and synchronous $H\alpha$ monochromatic photographs

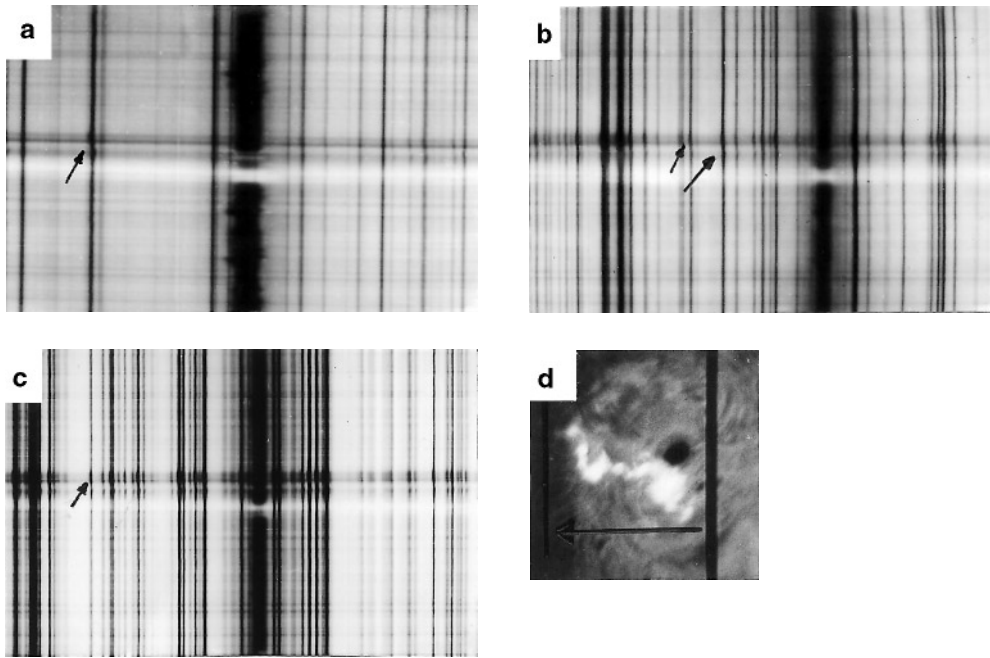


Fig. 1a–d. Spectral data (*a* $H\alpha$, *b* $H\beta$ and *c* $H\gamma$) and morphology of the flare of 5 July 1989. The thick black line in *d* is the spatial location of the incident slit when the flare begins to be scanned

Table 1. The flare of 5 July 1989 and associated emission

Time (UT)			Type of emission	Importance
Start	Max.	End		
0601		0750	Radio emission (continuum)	
0753E	0756	0829	X-ray	C9.6
0753	0800	0829	$H\alpha$	1N

by using the solar two-dimensional multi-band spectrograph equipped with an $H\alpha$ slit-jaw monitor system at Yunnan Observatory (Xuan & Lin 1993). From 0924UT to 0925UT, the two-dimensional scanning data of the longitudinal magnetic field of the active region (the selected sensitive line is $\text{Fe I } \lambda 6173 \text{ \AA}$) were obtained by using the same apparatus (Zhong and Xuan 1989; Zhong et al. 1992). We observed this flare by means of scan-photography, the scan step was $5''$. The film used in this observation was Kodak 2415. Exposure time for $H\alpha$ monochromatic photographs is $1/30$ s and for spectral photographs: 0.2 s for $H\alpha$, 0.5 s for $H\beta$, 0.5 s for $H\gamma$, 1 s for $\text{Fe I } \lambda 6173 \text{ \AA}$ respectively. The spectral data were measured using the PDS microdensitometer of Purple Mountain Observatory. Some data of the flare and associated emissions (NOAA 1989, 1990) are listed in Table 1.

Table 1 indicates that (1) the flare occurs in a higher layer of the solar atmosphere, namely about in the corona layer, then extends downwards to the chromosphere; (2) the burst in flare emission occurs simultaneously with the X-ray burst, which implies a rapid excitation (Tandberg-Hanssen & Emslie 1988); (3) the radio continuum emission ended several minutes later than the beginning of the flare, and after then, no radio emission

was recorded. This indicates that there is possibly no or very few electron beams with high energy in the solar corona hitting the photosphere to produce the continuum emission of the flare. There are two events: an Arch Filament System (or an Active Dark Filament) and Dark Surge on the Disk over the active region a few days before and after the beginning of the flare. During the active region's transit, 25 flares of SN class or SF class occur in the active region before the beginning, 19 flares of SN or SF class occur in the active region after the beginning (NOAA, 1990). The flare has several eruptive centres and four brighter spots (kernels). The flare overlaps the following sunspot in the active region.

3. Identification of the flare as a WLF

3.1. Events with continuous emissions

The solar flare radiation in the visible light wavelength band usually enhances the line-centre intensity and widens the line width only in the sensitive spectral lines (e.g. $H\alpha$, $H\beta$). The broadened width is approximately from 1.8 \AA to 8.8 \AA , with an average of 3 \AA (Svestka 1976; Hu et al. 1983). Generally, a continuous emission is hard to detect for a solar flare in the visible light wave band and occurs only when rare phenomena (including WLFs) take place. Events with continuous emissions are (1) bright photospheric faculae near the solar limb; (2) the 'moustache' phenomenon; (3) WLFs (Bruzek 1972; Svestka 1972; Hu et al. 1983; Chen & Wang 1984; Hiei 1986, 1993; Zhong et al. 1991; Xuan et al. 1992). The prominent difference between WLFs and the others is that only WLFs emit at line centers.

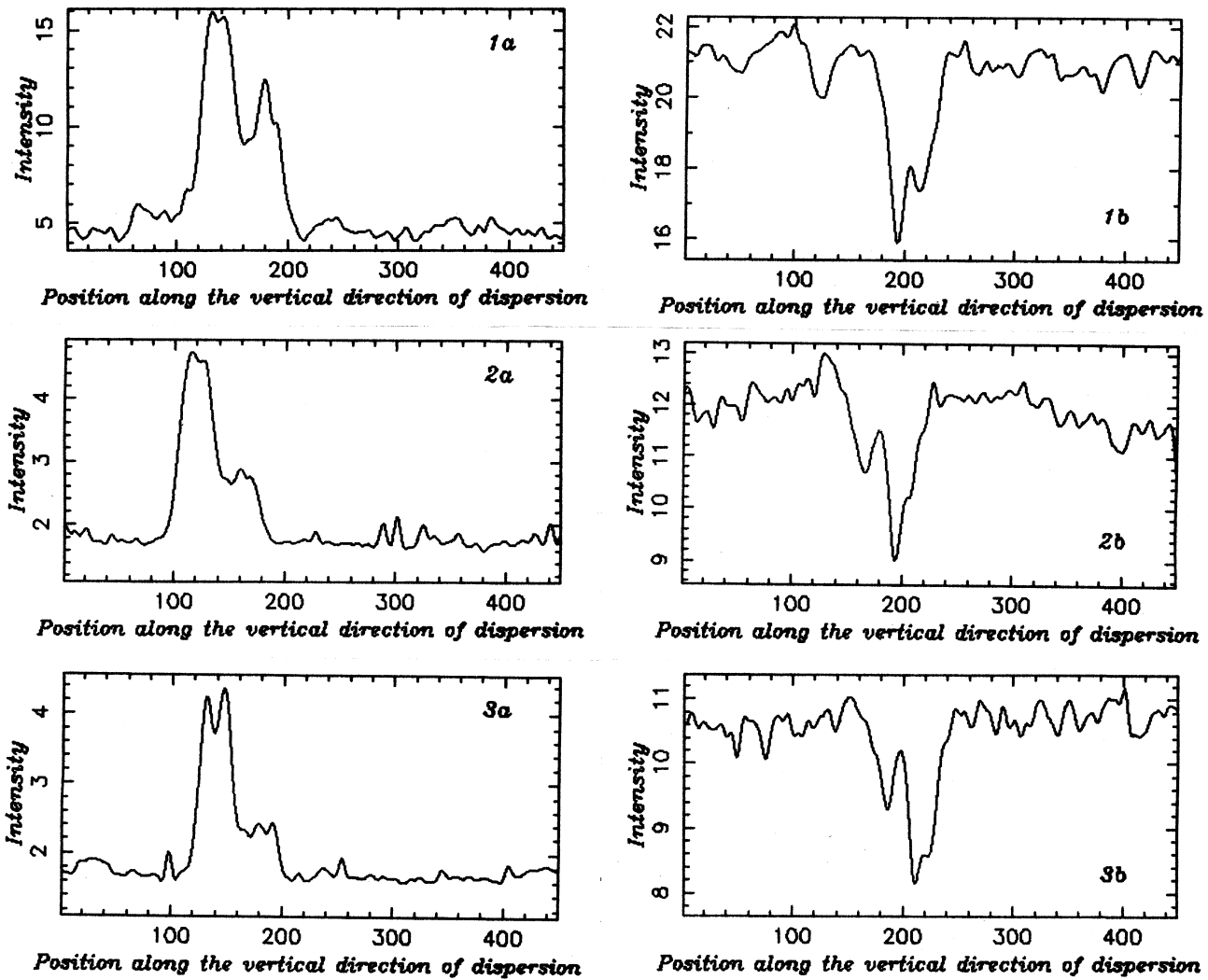


Fig. 2a and b. Profiles of intensities along the direction perpendicular to the dispersion. Symbol a indicates that intensities are measured at the line centres and symbol b at the outskirts. Symbol 1 corresponds to H α spectrum, 2 to H β , and 3 to H γ

3.2. Identification of the flare as a WLF

The H α flare has four bright spots (kernels). Figure 1 gives the spectral data of the brightest kernel, showing that the continuous emission band (white bands on the photograms of the figure) stretches across the entire spectral images of H α , H β , and H γ respectively. The dispersion range is 21 Å for H α , 25 Å for H β , 26 Å for H γ , respectively. The wavelengths of all these continuum emissions are more than 20 Å. The two-dimensional scanning spectral data show that each of the four flare kernels has a continuum. Figure 1d shows the scanned area, the direction of scanning (marked with arrow), and the slit image (the thicker black line in the figure).

The spectral data given in Fig. 1 are processed, and lines of intensity varying along the direction perpendicular to the dispersion are given in Fig. 2. Two cases are shown one with the data measured at the line centre and the other at a place away from the line centre.

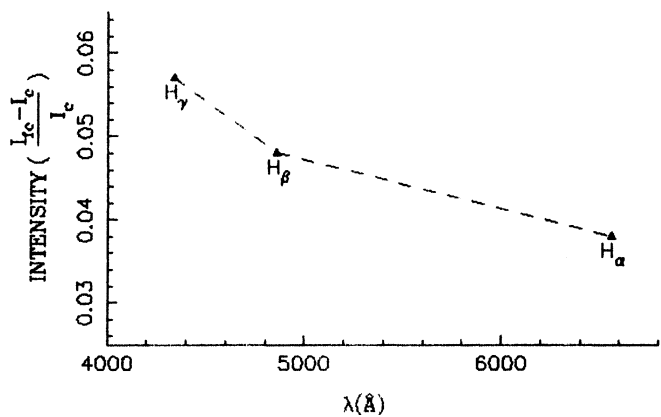


Fig. 3. The relative intensity of the brightest kernel

Figure 3 is based on Fig. 2. I_k and I_c are intensities of the kernel's continuum and of the background in the vicinity of the

flare, respectively. The curve is similar to that obtained by Boyer et al. (1985).

Unfortunately, the spectral scan (0758UT) began about 5 min later than the beginning of the flare (0753UT), so the onset time of the continuous emission is unknown. During the scanning (0806–0807UT), the continuous emission was very weak, and the flare kernels gradually disappeared, so we estimate the life-time of the continuous emission at less than 15 min (0753–0807UT). The sunspot class of the sunspot group in the active region is Dai type for morphology, β type for the magnetic field. The $H\alpha$ flare is sinuous and overlaps part of the preceding sunspot and all of the following one (see Fig. 1). The analyses of the magnetic field show that three of the four flare kernels in the $H\alpha$ flare are located in two penumbrae, of the two main sunspots, and the positions of all of them are near the umbrae. That the fourth kernel is located far from the two main sunspots and near a very small sunspot is an interesting phenomenon.

To sum up, the spectral characteristics, locations, duration, timing, configurations of the flare kernels are similar to those of a WLF, so the flare (or the four flare kernels) is very likely to be a WLF. The total energy radiated in $H\alpha$ in the WLF can be comparable to the continuum radiation (Slonim & Korobova 1975). It can be assumed that the energy radiated in the continuum is about half of the total energy. For the WLF on 5 July 1989, the total area of the four flare kernels is about $2.4 \times 10^{17} \text{ cm}^2$, life-time of the four flare kernels is about 800 s. Taking the flux of a bright WLF kernel as $1.0 \times 10^{10} \text{ ergs}^{-1} \text{ cm}^{-2}$ (Neidig 1989), then the total energy E_t is estimated to be:

$$E_t = 2 \times 1.0 \times 10^{10} \times 2.4 \times 10^{17} \times 800 = 3.84 \times 10^{30} \text{ erg}$$

3.3. Movement of the flare

The morphology of the flare has little obvious variation during its occurrence, so the horizontal velocity of the flare is small. The spectral diagnoses indicate that the velocity along the line of sight is small too, about several kilometers per second with both red shift and blue shift. The line-of-sight velocity of the flare kernels is not large, less than 20 km s^{-1} with red shift only, no blue shift is observed for the flare kernels.

Other points: The two black or grey bands near the white continuum band in each of the $H\alpha$, $H\beta$ and $H\gamma$ spectral images of Fig. 1 are spectra of the two main sunspots, and the spectral lines between the two bands in each image incline (see the lines marked by arrow in pictures (a), (b) and (c) of Fig 1). One end of the oblique line is of red shift, and the other end is of blue shift. This may be caused by Zeeman splitting, but there are many lines, which are insensitive to the magnetic field inclining as well, so the Zeeman effect is very small. The position of the spectrograph slit during the exposures indicates that the two black or grey bands are the continua of very small parts of both the following and preceding main spots. The slit covered small parts of their penumbrae. The observed shifts (about 7 km s^{-1}) might be caused by the Evershed effect or a 'reversed' Evershed effect in both spots, because the greatest changes in spot activity

occurred here, and connected with anomalous distributions of Doppler motions (about zero to 6 km s^{-1}).

4. Analysis of the magnetic field

WLFs are related to the magnetic field (Zirin 1988). Hiei et al. (1986) pointed out that the magnetic field of the brightening patch of a WLF completely shears. The study of Gesztelyi et al. (1985) made it known that the magnetic field of a WLF shears and twists and a WLF is usually produced in δ -structure sunspots. Bumba & Gesztelyi (1988) thought that production of a WLF is related to the large-scale distribution of the solar background magnetic field. Although much work has been done to understand the relation between WLFs and the magnetic field, a detailed quantitative analysis of the magnetic field data of a WLF has not been given up to now.

The trend of penumbra fibres of a sunspot may be regarded as the run of the transverse magnetic field of the sunspot (Danielson 1961). Figure 4 gives an image of the sunspot group in AR5575 at 0724UT on 5 July 1989, whose location is $N23^\circ E39^\circ$ on the solar disk. Also shown are distribution of sunspot polarity (a normal polarity distribution) the trend of penumbra fibres of the main sunspots in the active region, and the contour of the longitudinal magnetic field measured by using $\text{Fe I } \lambda 6173 \text{ \AA}$ with the spectra-spectroheliograph during 0924UT to 0925UT (Zhong & Xuan 1989; Zhong et al. 1992). The basic characteristics of the magnetic field are (a) the strength and area of the longitudinal magnetic field are larger for the preceding sunspot with negative polarity than those for the following sunspot with positive polarity. The maximum field strength is 2100 Gs for the preceding sunspot, 1200 Gs for the following sunspot, and the two strongest magnetic areas are immediate neighbours, the distance between them being about $9''$. (b) In the vicinity of the two main sunspots, the neutral line of the magnetic field $H_{//} = 0$ is nearly parallel to the isopleths of the longitudinal magnetic field and looks like the letter U or V with inclination about 60° . (c) The gradient of the magnetic field is the largest in the vicinity of the V-shape line. Along the axial line which joins the two main sunspots, the gradient is an average of 0.46 Gs km^{-1} for the region of the preceding sunspot and 0.4 Gs km^{-1} for the region of the following sunspot. Along the axial line away from the two sunspots, the gradient is less than 0.25 Gs km^{-1} for the preceding sunspot, less than 0.3 Gs km^{-1} for the following sunspot. That the latter two values are less than the former two values indicates that the two magnetic regions with opposite polarities were possibly compressed, and that this compression produced the V-shape in the neutral line of the magnetic field and different gradients of the magnetic fields between and out of the two main sunspots. (d) We can discern the penumbra fibrils of the two main sunspots from their photograph, and the fibrils are sketched in Fig. 4c. The trend of the penumbra fibres from the umbra to the limb of the preceding sunspot is a whirlpool shape. The magnetic line may be helical clockwise. The opposite case occurred in the following sunspot. From the inclinations of fibres of the two penumbrae, the following sunspot is perhaps spiraled

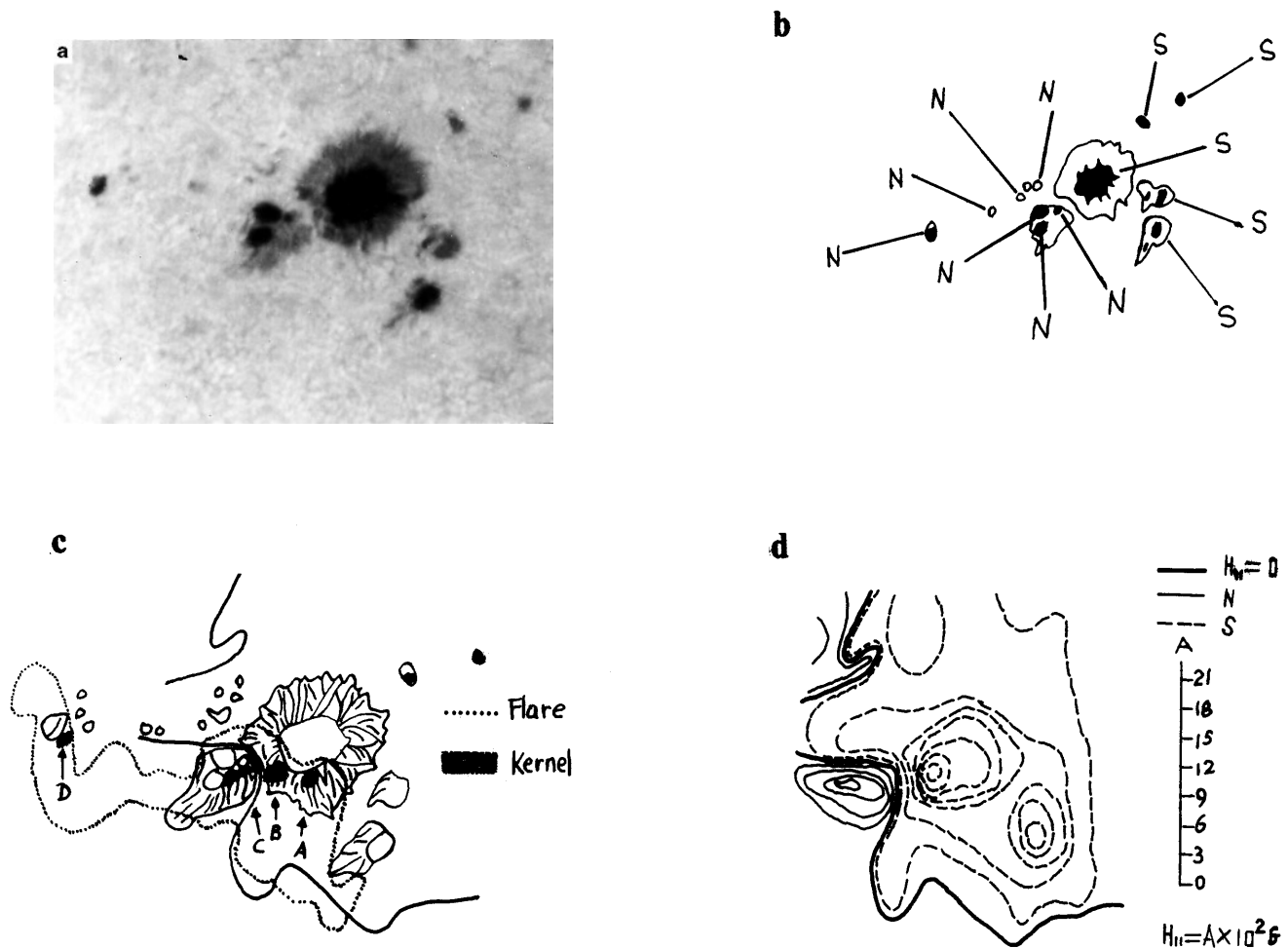


Fig. 4a–d. The morphology and the magnetic field of the active region: **a** the morphology of the active region, **b** the map of sunspot polarity, **c** schematic diagram of the transverse magnetic field, **d** contour of the longitudinal magnetic field

faster than the preceding sunspot. According to the result of the spectral analyses of the two main sunspots, we estimate that material in the preceding sunspot may rotate counterclockwise in descending, while material in the following sunspot may rotate clockwise in rising. This result is only a suggestion, but the material in the two main sunspots must go up or down along the magnetic lines, and cannot go across the heliocentric magnetic lines. At the place which joins the limb of the two main sunspots, the trend for both the transverse magnetic fields is nearly parallel to the neutral line. This characteristic is especially more obvious for the following sunspot. So the magnetic field of the active region perhaps shears and twists according to the above description.

Among the four flare kernels, the brightest one is kernel B (see Fig. 4), the secondary one is kernel C, and the third is kernel A. Magnetic fields which correspond to the four kernels are described as:

Kernel A: Its size is about $2.5''$. It is located within the penumbra of the preceding sunspot and extends to the umbra. The field strength of the active region around the kernel is in the range of

900 to 1500 Gs, the magnetic gradient is about 0.22 Gs km^{-1} . The magnetic field twists, and it is squeezed.

Kernel B: about $5.6''$ in size. Its field strength varies from 0 to 1800 Gs. The gradient of the magnetic field is the largest: 0.52 Gs km^{-1} . Obviously, the magnetic field shears and twists, and it is squeezed.

Kernel C: about $8''$ in size. It is located beside the neutral line and extends to the umbra of the following sunspot. Its field strength varies from 600 Gs to 1200 Gs. The gradient is 0.12 Gs km^{-1} . The magnetic field shears and twists, and it is squeezed too. Kernel C and Kernel B are symmetrically located on either side of the neutral line.

Kernel D: about $2.4''$ in size. It is located in the photospheric region and near a small sunspot whose size is about $4''$. There is no datum of the magnetic field for the kernel.

5. Discussion and conclusions

The continuous emission spectra of $H\alpha$, $H\beta$ and $H\gamma$ wavelength bands of the solar flare on 5 July 1989 are given and analysed. The study shows that the characteristics of the spectra, the lifetime, the size, and the configuration of each of the flare kernels in the flare are similar to those of a WLF, and therefore the flare is very likely to be a WLF. According to the spectral diagnoses of the flare, the line-of-sight velocities of the flare are small, about several kilometers per second with red shift or blue shift for $H\alpha$ lines and seem to decrease roughly in an order of $H\alpha$, $H\beta$, and $H\gamma$. The velocities of the four flare kernels are generally less than 20 km s^{-1} and only with red shift. The contrast $(I_{fc} - I_c)/I_c$ shows that solar WLFs are usually 'blue', as usually occurs in stellar flares. The reason why the brightness increases at short wavelength was described by Neidig (1989). The total radiation energy of the flare is about $3.84 \times 10^{30} \text{ erg}$.

In this paper, the magnetic field of the active region which encloses the flare is analysed. The field strength of the active region varies from -2100 Gs to $+1200 \text{ Gs}$. Squeezing of the two magnetic regions usually causes the neutral line of the magnetic field between the two regions with opposite magnetic polarities to assume an S-shape (Ai & Kong 1982) or V-shape, which happened to AR5575 which enclosed the flare on 5 July 1989. Three of the four kernels in the flare are situated at either side of the neutral line of the magnetic field. The observational result that flare kernels are situated at either side of the neutral line of the magnetic field has been found more than thirty years ago by the Crimean group. The fourth kernel of the flare is situated in the photospheric region and near a small sunspot (about $4'$ in size), which is an interesting phenomenon. The flare kernel with the most obvious continuous emission is situated at the point of intersection between the magnetic shearing and extruding lines, where there is maximum gradient of the magnetic field ($0.52 \text{ s Gs km}^{-1}$) and where the magnetic field shears and twists, and is squeezed. Magnetic fields of WLFs seem to be of two kinds: either the magnetic field twists, shears, and is squeezed (e.g. kernels A, B, and C of the flare), the other or that a WLF emerges in the photospheric region near the sunspot group or a sunspot (e.g. kernel D of the flare). In this case, the WLF possibly relates to the entire background magnetic field (Bumba & Gesztelyi 1988) or something else as gets unknown.

According to the morphology and spectrum of a sunspot group, one can determine its motion. In this paper, we determine the material in the preceding sunspot in the active region NOAA/USAF 5575 to go down to the lower solar atmosphere layer with velocity about 7 km s^{-1} , completely opposite motion with the same velocity in the following sunspot.

We will study the characteristics of the line profile, the line-of-sight velocity field and other parameters, spatial structure and evolution of this white light flare in detail in a future paper.

Acknowledgements. This work was supported by both the President Foundation of the Chinese Academy of Sciences and the Youth Foundation of Yunnan Province of P.R.China. The authors are much obliged to the Chinese Academy of Sciences and the Science and Technology Committee of Yunnan Province for their financial support. We would

like to thank the PDS staff at Purple Mountain Observatory for their help in digitising the spectral data on films and also thank Dr. Cao Yin, Prof. Ding Youji, Dr. Ding Jiang and the staff of the VAX-8350 Computer Group at Yunnan Observatory for their help and support.

References

- Aig G.X., Kong F.X., 1982, *Acta Astronomica Sinica* 23, 211
 Boyer R.M., Machado M.E., Rest D.M., Sotirovski P., 1985, *Solar Phys.* 98, 255
 Bruzek A., 1972, *Solar Phys.* 26, 94
 Bumba U., Gesztelyi, L., 1980, *Bull. Astron. Inst. Czech.* 39, 86
 Bumba U., Gesztelyi, L., 1988, *Bull. Astron. Inst. Czech.* 39, 1
 Chen Xiezheng, Wang Zhenyi, 1984, *Acta Astronomica Sinica* 25, 127
 CSGD editorial group, 1989, *China Solar-Geophysical Data* 6-7, 30
 Danielson R.E., 1961, *ApJ* 134, 289
 Gesztelyi L., Karlicky M., Franik F., Gerlei O., Valnicek B., 1986, In *The Lower Atmosphere of Solar Flares, Conference Proceedings*, ed. Neidig D.F. (USA: National Solar Observatory), 129
 Hiei E., 1986, *Adv. Space Res.* 6, 227
 Hiei E., 1993, In *Proceedings fo the First China-Japan Seminar on Solar Physics*, ed. Ai G.X., Hiei E., Ding Y.J., Ling Z.X. (China: Kunming TonDar Institute) 118
 Hiei E., Zirin H., Wang Jj, 1986, In *The Lower Atmosphere of Solar Flares, Conference Proceedings*, ed. Neidig D.F. (USA: National Solar Observatory), 129
 Hu Wenrei, Lin Yuanzhang, Wu Linxiang, 1983, in *Solar Flares (China: Science Press*, 70
 Lites B.W., Cook J.W., 1979, *ApJ* 288, 598
 Machado M.E., Avrett E.H., Vernazza J.E., Noyes R.W., 1980, *ApJ* 242, 336
 Neidig D.F., 1989, *Solar Phys.* 121, 261
 Neidig D.F., Cliver E.W., 1983, *Solar Phys.* 88, 275
 Neidig D.F., Wiborg P.H., 1993, *Solar Phys.* 144, 169
 NOAA, 1989, *Solar-Geophysical Data, Prompt Reports, Part I*, 541, 122
 NOAA, 1990, *Solar-Geophysical Data, Comprehensive Reports, Part II*, 545, 7
 Slonim Y.M., Korobova Z.B., 1975, *Solar Phys.* 40, 397
 Svestka Z., 1976, *Solar Flares*, ed. McCormac B.M. (Holland: D. Reidel Publishing Company), 81
 Svestka Z., 1972, *Annual Review of Astron. and Astrophys.* 10
 Tandberg-Hanssen E., Emslie A.G., 1988, *The Physics of Solar Flares* (Cambridge: Cambridge University Press), 226
 Wang Jingzi, Shen Longziang, Fang Chen, 1986, *Progress in Astronomy* 4, 175
 Worden S.P., 1983, *Activity in Red Dwarf Stars*, ed. Byrne P.B., Rodono M. (Holland: D. Reidel Publ. Co.), 207
 Xuan J.Y., Lin J., 1993, *Solar Phys.* 144, 307
 Xuan Jiayu, Zhong Shuhua, LuoZhi, Lin Jun, Ye Huilian, Chen Xuekun, 1992, *Chinese Science Bulletin* 37, 391
 Zirin H., 1988, *Astrophysics of the Sun* (Cambridge: Cambridge University Press), 401
 Zhong S.H., Xuan Y.J., 1989, *Publications of Yunnan Observatory* 4, 18
 Zhong Shuhua, Chen Xuekun, Luo Zhi, 1991, *Publications of Yunnan Observatory* 2, 14
 Zhong Shuhua, Luo Zhi, Xuan Jiayu, Lin Jun, 1992, *Publications of Yunnan Observatory* 1, 42